An Approximate Formulation for Scattering by Very Thin Dielectric Scatters

얇은 유전체의 산란특성 해석을 위한 근사식

Il-Suek Koh

고 일 석

Abstract

In this paper, a novel approximate solution for scattering by a very thin planar homogeneous dielectric scatterer with an arbitrary shape is formulated. This solution is based on a volumetric integral equation and is expressed in terms of Fourier transform. It is shown that the obtained solution is reduced to an exact solution for an infinite dielectric slab. For 2D, or 3D scatterers, the formulation is verified numerically. Especially for edge-on TM polarized wave incidence a closed-form solution of backscattering from a thin dielectric half-plane is formulated, which is very accurate for wide range of normalized surface impedance except very low impedances($|\eta|<0.5$).

요 약

본 논문에서 얇은 균질 유전체의 산란해석을 위한 근사식이 유도된다. 이 해는 volumetric integral equation을 바탕으로 Fourier transform 형식으로 나타내어진다. 얇은 무한 평면구조에서는 구한 식은 정확한 해로 떨어지며 다른 2D 또는 3D 구조에 대해서는 수치해석 결과와 비교하여 구한 식의 유용성을 보였다. 특히 TM파가 edge-on 방향으로 입사할 경우 반 무한 평면 구조에서의 산란에 대한 closed-form식을 구했다. 구한 식은 넓은 범위의 유전률에 대해 정확한 결과를 예측한다.

Key words : Scattering, Dielectric Half-Plane, Dielectric Disk

Ⅰ. Introduction

Scattering from a very thin dielectric is a classic research topic in electromagnetics and has found many applications. Usually, this kind of structure has been modeled with a resistive sheet, and for several geometries of this structure, exact solutions are known[1]. For example, solutions for scattering from a resistive half-plane can be obtained using the Wiener-Hopf technique or dual integral equation formulation, which are represented in terms of Maliuzhinets half-plane function. For other geometry such as a finite disk an exact solution is not yet known[2]. Therefore to this structure, a numerical method such as method of moment(MoM) or approximate analytical solutions such as physical optic(PO) or physical theory of diffraction(PTD) to include an edge diffraction effect should be applied.

A thin dielectric disk is widely adopted for a model of broad leaves of a deciduous type tree[3],[4]. To accurately estimate characteristics of forest channel such as backscattering, attenuation, etc., it is very important to increase the accuracy of scattering from leaves[5],[6]. For

인하대학교 정보통신대학원(The Graduate School of Information Technology and Telecommunication, Inha University)
· 논 문 번 호 : 20040522-05S
· 수정완료일자 : 2004년 7월 28일

this kind of structure two approximate solutions, volumetric integral physical optics(VIPO) and Rayleigh-Gans PO, are usually used, but the accuracy of these two PO approximations is strongly dependant on the size and thickness of a leaf, frequency, dielectric constants, and incidence angles, etc[5]. Rayleigh-Gans PO is valid when the thickness is sufficiently small ($|k_0 t\sqrt{\varepsilon_r - \sin^2\theta_i}| << 1$, see Fig. 1). VIPO can generate accurate results independent of the thickness, but always approaches zero for edge-on incidence. Therefore with increasing frequency or/and for a near-grazing incidence case, the accuracy of the existing methods is degenerated, and the computational complexity and the required size of memory for numerical methods like MoM drastically increase. Hence another analytical solution for scattering is required.

The volumetric equivalent theorem has been well-formulated and used intensively[7]. As pointed out in [8] the volumetric integral equation has not been used with MoM algorithm, except in the case of inhomogeneous scatterer problems, because it requires more memory than surface integral type formulations. However, the integral equation has been used to obtain an approximate solution for a polarization current inside a dielectric scatterer based on the well-known Neumann (Born) series approach[9],[10]: rough surface problems [11],[12] are one such example. However, it is very hard to formulate higher order terms using this kind of successive approximation type of method. Hence in this paper, another approximate solution is proposed, which is expressed in a simple form, but contains partial properties of higher terms of the Born series. Therefore, the proposed solution is valid for a wider range of dielectric constants, and incidence angles, etc. than the conventional approximate solutions. In Section 2, a polarization current inside a scatterer and a resulting electric field radiated by the current are formulated for an arbitrarily shaped 3-D planar structure. Then in successive Sections, the obtained solutions are verified analytically or numerically for several structures. For this paper, $e^{-i\omega t}$ is assumed.

Ⅱ. Formulation

Fig. 1(a) shows the problem geometry in which a very thin dielectric scatterer is located in a xy plane, and its surface is perpendicular to z-axis. This scatterer has a thickness of t, and a dielectric constant of ε_r, which is constant over the scatterer(homogeneous). According to the volumetric equivalent theorem, the scatterer can be replaced with the host medium(ε_0) and a polarization current of $\vec{J}(x,y,z)$, which satisfies the following equation known as the volumetric integral equation.

$$\vec{J} - k_0^2(\varepsilon_r - 1)\int_V \bar{\bar{G}}\,\vec{J}dv' = -ik_0 Y_0(\varepsilon_r - 1)\vec{E} \quad (1)$$

where k_0 is the free space wave number, $Y_0 = 1/Z_0$, Z_0 is the free space wave impedance, $\vec{E}^i$ is an incident wave, and $\bar{\bar{G}}$ is the free-space dyadic Green's function[9],

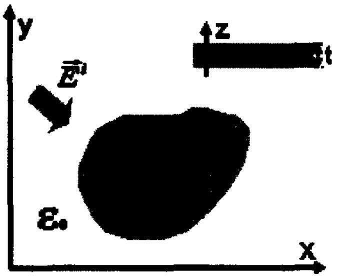

(a) Original geometry

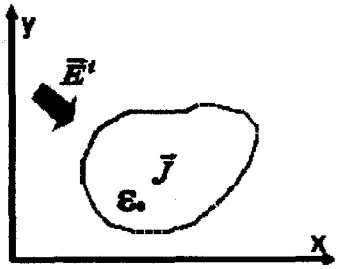

(b) Equivalent problem after applying the volumetric equivalent theorem

Fig. 1. Problem geometry: A very thin dielectric disk is located in a xy plane, and its normal is z-axis.

which is expressed in spectral domain as,

$$\bar{\bar{G}}(\vec{r},\vec{r}') = -\hat{z}\hat{z}\frac{\delta(\vec{r}-\vec{r}')}{k_0^2} + \frac{i}{8\pi^2}\int\int_{-\infty}^{\infty} d^2k \frac{e^{i[k_x(x-x')+k_y(y-y')]}}{k_z} \cdot \begin{cases} \left[\hat{h}\hat{h}+\hat{v}_+\hat{v}_+\right]e^{ik_z(z-z')} & \text{if } z > z' \\ \left[\hat{h}\hat{h}+\hat{v}_-\hat{v}_-\right]e^{-ik_z(z-z')} & \text{if } z > z' \end{cases} \tag{2}$$

where $k_x^2+k_y^2+k_z^2=k_0^2$, and $\hat{h}$, $\hat{v}_+$, and $\hat{v}_-$ are defined as

$$\hat{h}=\frac{\hat{k}^i\times\hat{z}}{|\hat{k}^i\times\hat{z}|},\ \hat{v}_+=\hat{h}\times\hat{k}^i,\ \hat{v}_-=\hat{h}\times\hat{k}^r$$

Here $\hat{k}^i=\frac{1}{k_0}(k_x^i\hat{x}+k_y^i\hat{y}+k_z^i\hat{z})$, and $\hat{k}^r=\frac{1}{k_0}(k_x^i\hat{x}+k_y^i\hat{y}+k_z^i\hat{z})$. It may be simply observed from (1) that both right- and left-handed sides in (1) are defined only inside the scatterer, due to the terms of ε_r-1 and the current($\vec{J}$) itself. By substituting (2) into equation (1) and then evaluating the delta term in (2) analytically, the volumetric integral equation (1) is expressed in a more compact form like

$$\vec{J}-Ak_0^2(\varepsilon_r-1)\int_{v'}\bar{\bar{G}}\cdot\vec{J}dv'=\vec{J}_{RG} \tag{3}$$

where $\bar{\bar{G}}_r$ is the integral part in (2), and $\vec{J}_{RG}$ is the well-known Rayleigh-Gans PO current[5], which is written as $\vec{J}_{RG}=-ik_0Y_0(\varepsilon_r-1)A\vec{E}^i$, and A is a diagonal matrix defined as $A=\hat{x}\hat{x}+\hat{y}\hat{y}+\frac{1}{\varepsilon_r}\hat{z}\hat{z}$. As seen in (3), the Rayleigh-Gans PO solution is the zeroth order solution of the modified volumetric integral equation. Hence the Rayleigh-Gans PO solution is valid when the integral part in (3) can be ignored.

As explained earlier, $\vec{J}$, and $\vec{J}_{RG}$ are defined only inside a scatterer(see Fig. 1), which can be expressed mathematically as

$$\vec{J}_{RG},\vec{J}(x,y,z)\begin{cases}\neq 0 & (x,y,z)\in\Omega \\ = 0 & (x,y,z)\notin\Omega\end{cases}$$

Therefore, when taking Fourier transform to the two currents, $\vec{J}$ and $\vec{J}_{RG}$, the infinite integral range is inherently truncated into a finite range of Ω as

$$\int\int\int_{-\infty}^{\infty}\vec{J}e^{i(k_xx+k_yy+k_zz)}dv'=\int\int\int_{\Omega}\vec{J}e^{i(k_xx+k_yy+k_zz)}dv' \tag{4}$$

Using this observation, an approximate solution of scattering from a thin dielectric disk will be developed. First the polarization current can be assumed as a function of only(x, y) and a constant with respect to z-axis because of the assumption of the thin thickness. Therefore, $\vec{J}(x,y,z)\approx\vec{J}(x,y,0)$. Hence in (3) the integral with respect to z can be evaluated using the mid-point rule. The result is given by

$$\int_{v'}\bar{\bar{G}}(\vec{r},\vec{r}')\vec{J}(\vec{r}')dv'\approx t\int_{s'}\bar{\bar{G}}_r(x,y,0;x',y',0)\cdot\vec{J}(x',y',0)ds' = \frac{t}{8\pi^2}\int\int_{-\infty}^{\infty}d^2k\frac{A\cdot L}{k_z}\vec{J}(x',y')e^{i[k_x(x-x')+k_y(y-y')]} \tag{5}$$

where L is approximated as

$$L\approx\frac{1}{2}[\hat{h}\hat{h}+\hat{v}_+\hat{v}_++\hat{h}\hat{h}+\hat{v}_-\hat{v}_-]=\frac{1}{k_0^2}\begin{pmatrix}k_0^2-k_x^2 & -k_xk_y & 0\\ -k_xk_y & k_0^2-k_y^2 & 0\\ 0 & 0 & k_0^2-k_z^2\end{pmatrix}$$

By substituting (5) into (3), (3) is rewritten as

$$\vec{J}-t\frac{k_0^2}{8\pi^2}(\varepsilon_r-1)\int\int_{-\infty}^{\infty}d^2k\vec{J}(x',y')e^{i[k_x(x-x')+k_y(y-y')]}=\vec{J}_{RG}$$

Using (4) the integral in the above equation is interpreted as a convolution integral. Hence with an approximation that the term of ε_r-1 extends to infinity, the above equation can be solved analytically, and the solution is written as

$$\int_s\vec{J}e^{-i(k_xx+k_yy)}ds\approx B^{-1}\int_{s'}\vec{J}_{RG}e^{-i(k_xx'+k_yy')}ds' \tag{6}$$

where $B^{-1}=\left[\bar{\bar{I}}-\alpha k_0^2\frac{A\cdot L}{k_z}\right]^{-1}$, $\bar{\bar{I}}$ is an unit dyadic, and $\alpha=\frac{i}{2}t(\varepsilon_r-1)$. B^{-1} can be expressed explicitly as

$$B^{-1}=\begin{pmatrix}\frac{1}{D}\left[k_z-\alpha(k_0^2-k_y^2)\right] & -\frac{\alpha}{D}k_xk_y & 0\\ -\frac{\alpha}{D}k_xk_y & \frac{1}{D}\left[k_z-\alpha(k_0^2-k_x^2)\right] & 0\\ 0 & 0 & \frac{\varepsilon_rk_z}{\varepsilon_rk_z-\alpha k_\rho^2}\end{pmatrix}$$

where $D=k_z(1+\alpha^2k_0^2)-\alpha(k_0^2+k_z^2)$, and $k_\rho^2=k_x^2+k_y^2$.

As explained before, the left-hand side in (6) can be interpreted as Fourier transform of $\vec{J}$, and so just by taking the inverse Fourier transform, a closed-form expression of $\vec{J}$ can be obtained and is given by

$$\vec{J}(x,y)=\frac{1}{4\pi^2}\int\int_{-\infty}^{\infty} d^2k e^{i(k_x x+k_y y)} B^{-1}\int_{s'}\vec{J}_{RG} e^{-i(k_x x'+k_y y')} ds' \tag{7}$$

It is expected that this solution may be accurate when the size of a scatterer is large or the integral contribution in (3) is small. For a plane wave incidence case, $\vec{E}=\vec{e}_i e^{i(k_x^i x+k_y^i y+k_z^i z)}$, the surface integral term in (7) is rewritten as

$$\int_{s'}\vec{J}_{RG} e^{-i(k_x x'+k_y y')} ds' = -ik_0 Y_0(\varepsilon_r-1)A\cdot\vec{e}_i\int_{s'} e^{i[(k_x^i-k_x)x'+(k_y^i-k_y)y']}$$

From the above representation of the polarization current, the electric field can be calculated, and is simply expressed especially in a far-field region as

$$\vec{E}\sim\frac{k_0^2}{16\pi^3}\frac{e^{ik_0 r}}{r}\hat{r}\times\hat{r}\times\int\int_{-\infty}^{\infty} d^2k B^{-1}\int_{s'} ds'\vec{J}_{RG} e^{-i(k_x x'+k_y y')}\cdot$$

$$\int_{s''} ds'' e^{-i[(k_x^s-k_x)x''+(k_y^s-k_y)y'']}$$

where $\hat{k}^s=\frac{1}{k_0}(k_x^s\hat{x}+k_y^s\hat{y}+k_z^s\hat{z})$ is an unit vector to an observation point. Due to a property of the Fourier transform, the surface integral in the above equation and (7) becomes narrower in spectral domain as the size of the scatterer increases(for an infinite scatterer, the integral becomes a delta function). Therefore, at high frequencies and/or for a large structure, the formulated equations are numerically very efficient.

Ⅲ. Infinite Dielectric Slab

To verify the obtained solution (7), first, an infinite dielectric slab is considered because an exact solution is known for this structure[5]. For this case, the formulation, (7), is exact. For simplicity, a plane wave is assumed to be incident, but the solution can be easily extended to a dipole excitation by the superposition principle. For this geometry, equation (7) can be evaluated analytically, and the final solution can be written in terms of a polarizability tensor like $\vec{J}=-ik_0Y_0(\varepsilon_r-1)[P_{xx}E_x^i\hat{x}+P_{yy}E_y^i\hat{y}+P_{zz}E_z^i\hat{z}]$. Here the incident wave is given by $\vec{E}^i=E_x^i\hat{x}+E_y^i\hat{y}+E_z^i\hat{z}$. After some algebraic manipulations, the elements of the polarizability tensor can be obtained as

$$P_{xx}=P_{yy}=\frac{k_z^i}{k_z^i-\alpha k_0^2},\ P_{zz}=0 \quad \text{for h-pol. incidence} \tag{8}$$

$$P_{xx}=P_{yy}=\frac{1}{1-\alpha k_z^i},\ P_{zz}=\frac{k_z^i}{\varepsilon_r k_z^i-\alpha k_\rho^{i2}} \quad \text{for h-pol. incidence} \tag{9}$$

where $k_\rho^{i2}=k_x^{i2}+k_y^{i2}$. Exact solutions[5] can be slightly modified to

$$P_{xx}=P_{yy}=\frac{2k_z^i}{\Delta_1},\ P_{zz}=0 \qquad \text{for h-pol. incidence}$$

$$P_{xx}=P_{yy}=\frac{2k_z'}{\Delta_2},\ P_{zz}=\frac{2k_z^i}{\Delta_3} \qquad \text{for v-pol. incidence}$$

where $\Delta_1=(k_z^i+k_z')e^{-i(k_z'-k_z^i)t/2}+(k_z^i-k_z')e^{i(k_z'+k_z^i)t/2}$, $\Delta_2=(\varepsilon_r k_z^i+k_z')e^{-i(k_z'-k_z^i)t/2}-(\varepsilon_r k_z^i-k_z')e^{i(k_z'+k_z^i)t/2}$, $\Delta_3=(\varepsilon_r k_z^i+k_z')e^{-i(k_z'-k_z^i)t/2}+(\varepsilon_r k_z^i-k_z')e^{i(k_z'+k_z^i)t/2}$, and $k_z'=\sqrt{\varepsilon_r k_0^2-k_\rho^{i2}}$. Due to the extreme thickness, the exponential terms in the above equations can be approximated by Taylor series expansion like $e^{i(k_z'+k_z^i)t/2}\approx 1+i\frac{t}{2}(k_z'+k_z^i)$. For an h-pol. incident case, therefore,

$$\Delta_1\approx 2k_z'+it(k_z'^2-k_z^{i2})=2k_z^i-2\alpha k_0^2$$

Using the above approximation, the exact P_{xx} can be reduced to (8). For a v-pol. incident case, the same results can be obtained by using the same approximation. Fig. 2 shows a plot of P_{xx} for a dielectric slab with two dielectric constants, $2+i$ and $20+i10$ as a function of incidence angles for the v-pol. incidence case. For this calculation, frequency and thickness are set to be 10 GHz and 0.2 mm, respectively.

Ⅳ. Dielectric Strip & Half-Plane

The next consideration concerns scattering from a

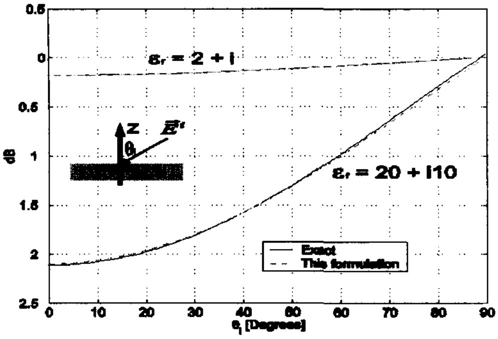

(a) Magnitude

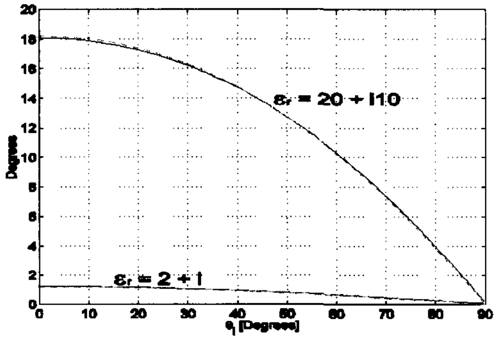

(b) Phase

Fig. 2. Plot of P_{xx} as a function of incidence angle when v-polarized wave is incident on an infinite dielectric slab with a thickness of 0.2 mm. Two different dielectric constants, ε_r=2+i and $20+i10$ are considered. Frequency is 10 GHz.

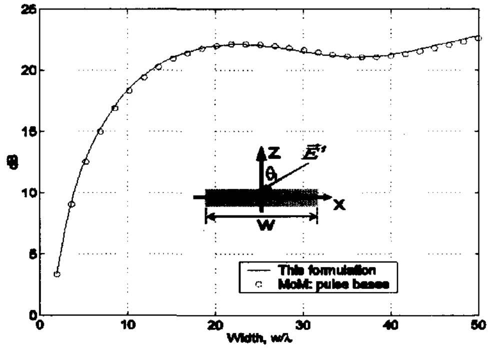

(a) Forward scattering

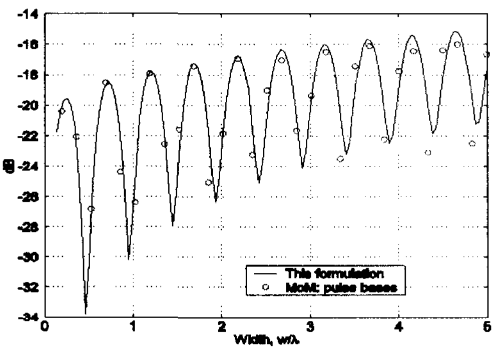

(b) Backscattering

Fig. 3. Plot of radar cross sections of a dielectric strip normalized by wavelength σ/λ_0 as a function of width for edge-on TM wave incidence case. Thickness of the strip is $0.025\lambda_0$, and the dielectric constant is $4+i0.4$.

thin dielectric strip. The geometry is shown in Fig. 3 (a). For a plane wave incidence case, the polarization current equation (7) can be reduced to a single integral representation as

$$\vec{J}(x,y) \approx -ik_0 Y_0(\varepsilon_r -1)\frac{w}{2\pi}\int_{-\infty}^{\infty} dk_x A\cdot\vec{e}_i B_1^{-1} e^{i(k_x x+k_y^i y)} \operatorname{sinc}\left[\frac{(k_x^i - k_x)}{2}w\right] \quad (10)$$

where B_1^{-1} is the B^{-1} with $k_y = k_y^i$, and $\operatorname{sinc}(x) = \sin(x)/x$. From this current representation, an electric field in a far-field region can be easily formulated as

$$\vec{E} \sim it(\varepsilon_r -1)\frac{(k_0 w)^2}{8\pi}\sqrt{\frac{2}{\pi k_0 \rho}}\, e^{i(k_0\rho-\pi/4)} \cdot \hat{r}\times\hat{r}\times\int_{-\infty}^{\infty} dk_x B_1^{-1}A\cdot\vec{e}_i \operatorname{sinc}\left[\frac{k_x^i - k_x}{2}w\right]\operatorname{sinc}\left[\frac{k_x - k_x^s}{2}w\right] \quad (11)$$

Unfortunately the above equation can't be evaluated into any closed-form expression. Hence to validate the equation numerically, examples are chosen from [13]. The thickness of the dielectric strip is set to be $0.025\lambda_0$, and the dielectric constant is $4+i0.4$. Fig. 3 shows comparisons of radar cross sections(RCS) from the strip that are calculated by this integral formulation and MoM with pulse basis function in forward and backward directions for an edge-on TM polarized incidence case. This computed RCS is normalized by wavelength. Fig. 4 shows a comparison of currents computed by (10) and MoM for the same situation as the RCS computation. For this calculation, the width of the strip is set to be $5\lambda_0$ and $50\lambda_0$. For the $50\lambda_0$ case only magnitude is plotted for an easy comparison, but it is observed that phase also is in excellent agreement.

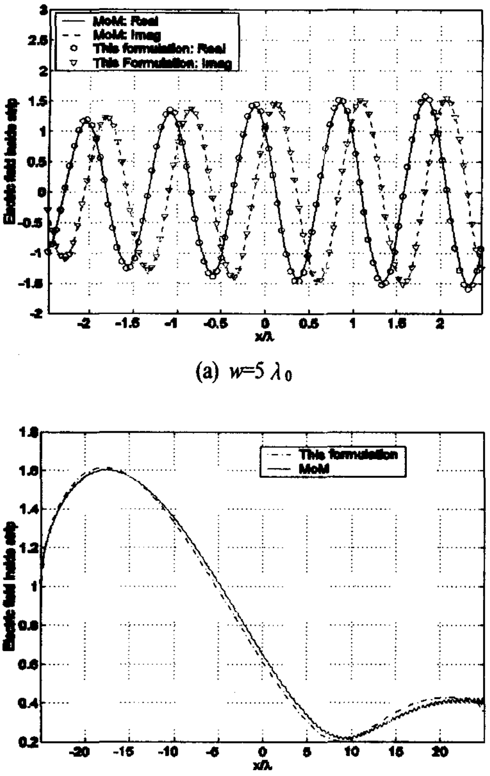

(a) $w=5\lambda_0$

(b) $w=50\lambda_0$

Fig. 4. Comparisons of polarization currents inside a dielectric strip with two widths, $5\lambda_0$ and $50\lambda_0$, which are computed by MoM and the new formulation for edge-on TM wave incidence case. Thickness of the strip is $0.025\lambda_0$, and the dielectric constant is $4 + i0.4$.

The next example is of backscattering from a thin dielectric half-space. For this structure, exact and approximate solutions are known [1, 14]. The problem geometry is shown in Fig. 5, in which a dielectric half-plane is located along a negative x-axis from the origin. For this geometry, (7) is reduced to

$$\vec{J}(x,y) \sim \frac{1}{2}\vec{J}_{\inf} - ik_0 Y_0(\varepsilon_r - 1)\frac{i}{2\pi}\int_{-\infty}^{\infty} dk_x A\cdot\vec{e}_t B_1^{-1}\frac{e^{i(k_x x + k_y^i y)}}{k_x - k_x^i} \tag{12}$$

where $\vec{J}_{\inf}$ is a current inside an infinite slab, which is PO current(See Section 3). The integral in (12) contains a singularity at $k_x = k_x^i$. If evaluating the pole contribution using a residue theorem, the complete PO current is obtained. If we focus on just edge-on incidence case, this PO current always becomes zero. For this paper, only the TM polarized wave is considered, which has only a y-component and $k_y^i = 0$. For a TE incidence case, a backscattering by a thin dielectric is very small, and the resistive sheet approach gives zero result[14]. Hence in this paper, only TM case is considered. In a far-field region, the electric field can be written in a form like $\vec{E} \sim \hat{y}\sqrt{\frac{2}{\pi k_0 \rho}}P_e(\theta_i,\theta_s)$. From (12) $P_e(\theta_i,\theta_s)$ can be computed for the backscattering direction as

$$P_e\left(\frac{\pi}{2},\frac{\pi}{2}\right) = \frac{k_0}{4\pi\eta}\int_{-\infty}^{\infty} dk_x \frac{1}{k_z(k_z - \alpha k_0^2)}$$

where $\alpha k_0 = -\frac{1}{\eta}$, and $\eta = \frac{2R}{Z_0}$ is the normalized surface impedance. The integral in the above equation can be evaluated into a closed-from expression, and so $P_e\left(\frac{\pi}{2},\frac{\pi}{2}\right)$ is rewritten as

$$P_e\left(\frac{\pi}{2},\frac{\pi}{2}\right) = -\frac{1}{\pi\sqrt{1-\eta^2}}\left[\tan^{-1}\frac{\eta-1}{\sqrt{1-\eta^2}} - i\tanh^{-1}\frac{\sqrt{\eta^2-1}}{\eta-i}\right]$$

$$= -\frac{i}{\pi\sqrt{1-\eta^2}}\tanh^{-1}\sqrt{\frac{1-\eta}{1+\eta}} \tag{13}$$

At $\eta = 1$ the above formulation may be computed analytically as $-\frac{i}{2\pi}$. An exact solution for a resistive half-plane is $-\frac{i}{4}\cdot 0.7894^2 = -i0.1558$. Hence a ratio of the new result to the exact one for the resistive half-plane is 1.0216, which is 2 % difference. To validate this formulation, a known asymptotic solution for a resistive half-plane problem is used [14]. For backscattering, $P_e\left(\frac{\pi}{2},\frac{\pi}{2}\right)$ is given by

$$P_e\left(\frac{\pi}{2},\frac{\pi}{2}\right) = -i\frac{\eta}{16}ZJ(0) \tag{14}$$

$ZJ(0)$ is represented by a contour integral including Maliuthinets half-plane function whose definition and approximations can be found in [1]. Fig. 5 shows a comparison of results calculated by (13) and (14) as a function of real η. As seen in Fig. 5 excellent agreement is observed. Discrepancy is increased with decreasing η because for this region, ε_r increases

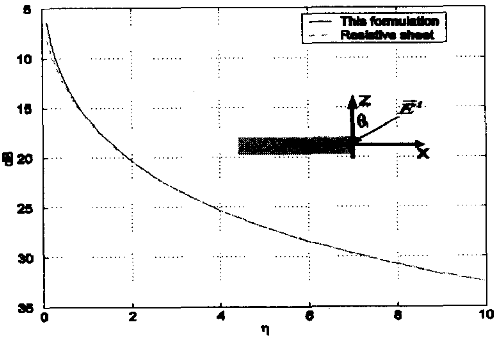

Fig. 5. Plot of backscattering(P_e) from a very thin dielectric half-plane as a function of real η for edge-on TM wave incidence case. Two results are compared, which are computed by the known asymptotic solution and the new formulation.

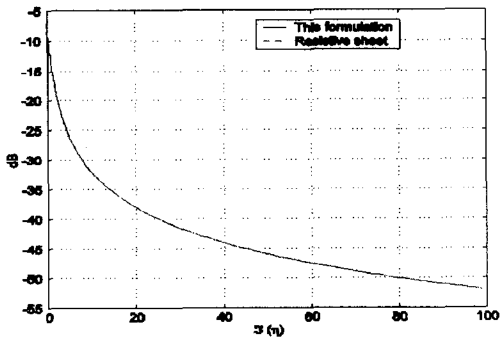

(a) Magnitude

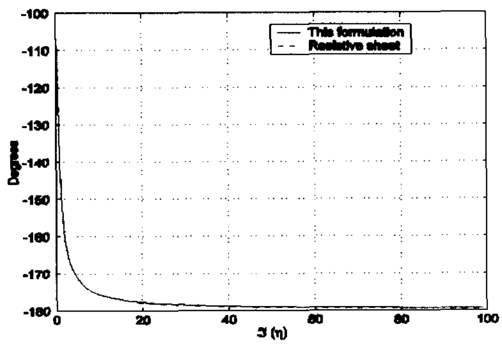

(b) Phase

Fig. 6. Comparisons of backscattering(P_e) from a dielectric half-plane which are computed by the new formulation, and the asymptotic solution. These are plots as a function of imaginary part of η with a fixed real part of 0.1.

and so contribution of the integral part in the volumetric integral equation becomes larger. For a perfect electrical conductor(PEC) case, η=0, this formulation is no longer valid because only the integral contribution exists in the volumetric equation. Fig. 6 is a plot of $P_e(\frac{\pi}{2},\frac{\pi}{2})$ as a function of the imaginary part of η and a fixed real part of 0.1. As seen in Fig. 6 the new formulation is matched well with the asymptotic results. As expected, a larger discrepancy is observed for smaller η. Hence (13) is a very good approximation for the Maliuthinets half-plane function for moderate and large $|\eta|$.

V. Dielectric Disk

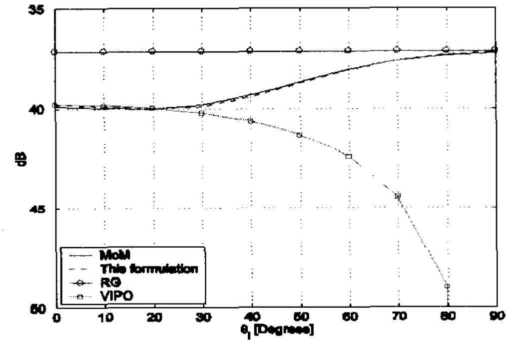

(a) Magnitude

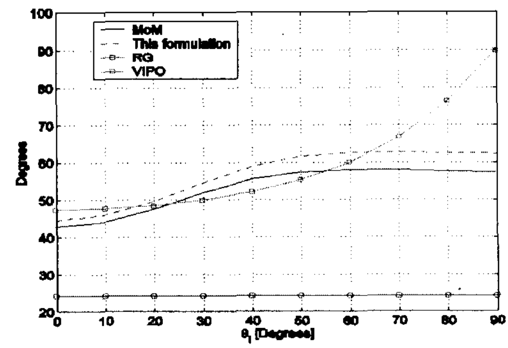

(b) Phase

Fig. 7. Comparisons of forward scattering of S_{hh} from a circular disk with a diameter of λ_0, thickness of 0.2 mm, and dielectric constant of $26.6 + i11.56$, which are computed by four methods such as the new formulation, MoM, VIPO, and Rayleigh-Gans PO. Frequency is 10 GHz.

In this section scattering by a very thin dielectric disk is examined. For this kind of geometry, the formulations derived in Section 2 can be directly used. First, scattering from a circular disk is investigated. Generally, exact evaluation of the surface integral in (7) is available for an ellipsoidal geometry[15]. When a and b are lengths of the ellipsoid along x-axis and y-axis, respectively, the integral can be evaluated in a closed-form expression as

$$\iint_{s'} e^{i[(k_x-k_x^i)x'+(k_y-k_y^i)y']}ds' = \frac{2AJ_1\left(\sqrt{a^2(k_x-k_x^i)^2+b^2(k_y-k_y^i)^2}\right)}{\sqrt{a^2(k_x-k_x^i)^2+b^2(k_y-k_y^i)^2}}$$

where $A=\pi ab$ is an area of the ellipsoid, and $J_1(\bullet)$ is the Bessel function of the first kind of order 1. For a circular disk, $a=b$. Since this structure is widely used for a model of broad leaves, for numerical simulations a real dielectric constant of that kind of leaf at 10 GHz of $26.6+i11.56$ is used for the dielectric constant of the disk. The first example is a calculation of the forward scattering from a disk with a diameter of λ_0, and a thickness of 0.2 mm. Fig. 7 shows a plot of forward scattering of S_{hh} from the circular disk as a function of incidence angles. As seen in Fig. 7 two approximate solutions such as VIPO and Rayleigh-Gans PO solutions can't generate accurate results, but the new formulation has very good agreement with MoM in the entire comparison region. Fig. 8 shows the same plots as Fig. 7 but frequency is increased to 20 GHz. As seen

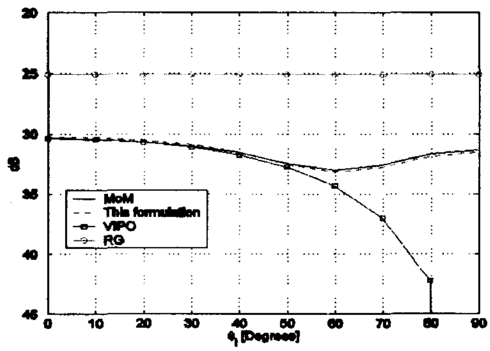

(a) Magnitude

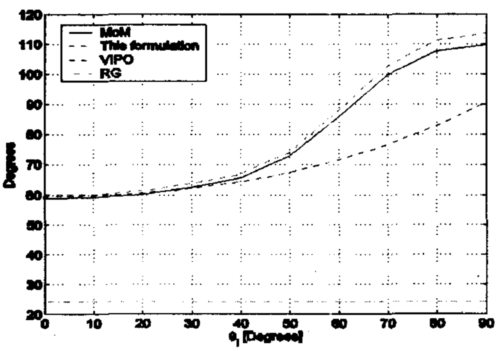

(b) Phase

Fig. 8. Comparisons of forward scattering of S_{hh} from a circular disk with a diameter of λ_0, thickness of 0.2 mm, and dielectric constant of $26.6+i11.56$, which are computed by four methods such as the new formulation, MoM, VIPO, and Rayleigh-Gans PO solution. Frequency is 20 GHz.

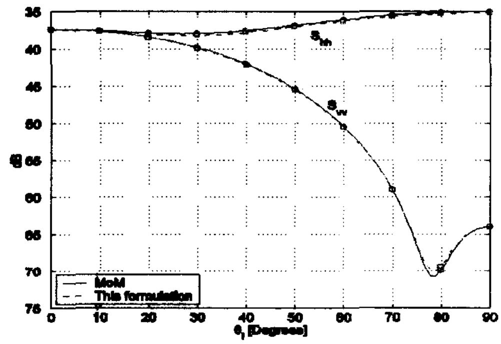

(a) Magnitude

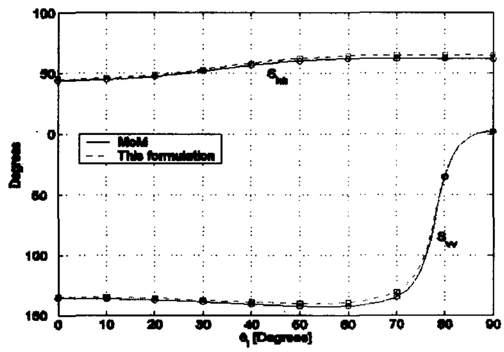

(b) Phase

Fig. 9. Comparisons of backscatterings of S_{hh}, and S_{vv} from a square disk with a width of λ_0, thickness of 0.2 mm, and dielectric constant of $26.6+i11.56$, which are computed by the new formulation and MoM. Frequency is 10 GHz. Lines are interpolated results, and "o" and "□" are originally calculated values.

in Fig. 8 the new formulation is matched very well with MoM again. The difference is less than 0.2 dB in magnitude, and 4° in phase for the two cases.

The next geometry is a square leaf. For this shape,

$$\iint_{s'} e^{i[(k_x-k_x^i)x'+(k_y-k_y^i)y']} ds' = w_x w_y \,\text{sinc}\left[\frac{k_x^i-k_x}{2}w_x\right]\text{sinc}\left[\frac{k_y^i-k_y}{2}w_y\right]$$

where w_x and w_y are widths of the square leaf along x- and y-axis, respectively. Fig. 9 shows a plot of back-scattering from a square leaf with a width of λ_0 and thickness of 0.2 mm as a function of incidence angles. For this calculation frequency is set to be 10 GHz. The maximum difference between two results is less than 0.2 dB in magnitude and 4° in phase. The next examination is about bistatic scattering from the same square disk. For this computation, a wave is incident from the negative x-axis($\phi_i = 180°$) at $\theta_i = 180°$(edge-on incidence). The observation point(θ_s) moves from −90° to 90° along the diagonal direction of the disk ($\phi_s = 45°$). Fig. 10 shows a plot of S_{hh}, and S_{vv} as a function of θ_s. These figures are results interpolated from originally calculated values at coarse points. Some discrepancy is observed in the backward direction. This error is caused by numerical error, because at the direction scattering is so weak. In the opposite direction, where scattering is strong, however, very good agreement is observed.

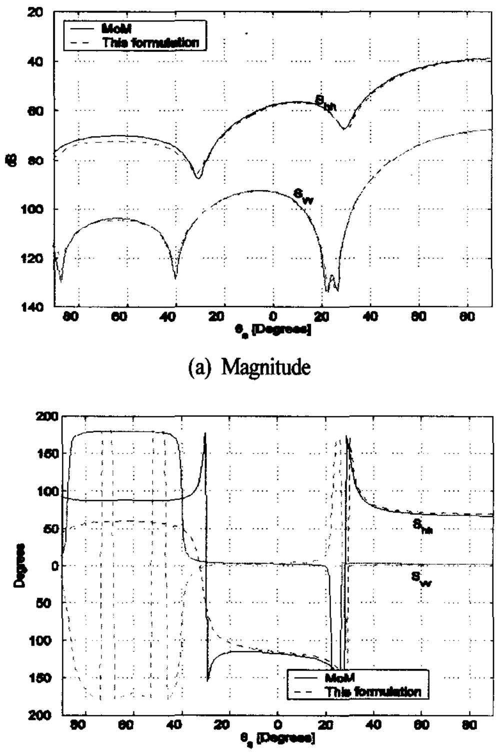

(a) Magnitude

(b) Phase

Fig. 10. Comparisons of bistatic scatterings of S_{hh} and S_{vv} from a square disk with a width of λ_0, thickness of 0.2 mm, and dielectric constant of 26.6 + i11.56, which are computed by the new formulation and MoM. Frequency is 10 GHz. θ_i is fixed to be 90°, and θ_s moves −90° to 90° with ϕ_i=180°, and ϕ_i=45°.

Ⅵ. Conclusions

In this paper, novel approximate formulations for scattering by a very thin homogeneous dielectric structure are developed. These formulations are derived based on a volumetric integral equation and the observation that polarization current is confined inside a scatterer only. Using the spectral domain representation of the free-space dyadic Green's function, the polarization current inside an arbitrarily shaped thin dielectric disk is expressed in a closed-form equation in spectral domain. For several structures, the formulated solutions are verified. For an infinite dielectric slab, it is shown that the exact solution can be reduced to the new formulation within the limit of small thickness. For 2D and 3D problems, thin dielectric half-space and strip, and circular and square disks are investigated. For these kinds of geometries, far-field characteristics such as forward, back, and bistaic scatterings are compared with results computed by MoM. Especially for a thin dielectric half-plane, a closed-form solution for back-scattering is formulated for edge-on TM wave incidence cases. This solution is compared with the known solutions for resistive half-planes, which shows very good agreement.

References

[1] T. B. A. Senior, J. L. Volakis, *Approximate Boundary Conditions in Electromagnetics*, Institution of Electrical Engineers, London, 1995.

[2] J. J. Bowman, T. B. A. Senior, P. L. E. Uslenghi and J. S. Asvestas, *Electromagnetic and Acoustic Scattering by Simple Shapes*, Hemisphere, New York, 1987.

[3] Y. C. Lim, K. Sarabandi, "Monte carlo coherent scattering model for forest canopies using fractal-generated trees", *IEEE Trans. on Geoscience and Remote Sensing*, vol. 37, no. 1, pp. 440-451, Jan. 1999.

[4] I. Koh, K. Sarabandi, "Polarimetric channel characteristics of foliage for performance assessment of gps receiver under tree canopies", *IEEE Trans. on Antenna Propagat.*, vol. 37, no. 1, pp. 713-726, May 2002.

[5] I. Koh, F. Wang and K. Sarabandi, "Estimation of coherent field attenuation through dense foliage including multiple scattering", *IEEE Trans. on Geoscience and Remote Sensing*, vol. 41, no. 5, pp. 1132-1135, May 2003.

[6] F. Wang, K. Sarabandi, "Theory and measurement of millimeter-wave propagation through foliage", *Submitted for Publication in IEEE Trans. Antennas Propagat.*

[7] R. F. Harrington, *Time-Harmonic Electromagnetic Field*, McGraw-Hill, New York, 1961.

[8] J. J. H. Wang, *Generalized Moment Methods in Electromagnetics: Formulation and Computer Solution of Integral Equations*, Wiley, New York, 1991.

[9] L. Tsang, J. Kong and R. T. Shin, *Theory of Microwave Remote Sending*, Wiley, New York, 1985.

[10] F. T. Ulaby, R. K. Moore and A. K. Fung, *Microwave Remote Sensing Active and Passive*, Arthech House, Norwood, 1982.

[11] K. Sarabandi, I. Koh, "Effect of Canopy-Air Interface Roughness on HF-UHF wave propagation in forest", *IEEE Trans. on Antenna Propagat.*, vol. 50, no. 2, pp. 101-110, Feb. 2002.

[12] K. Sarabandi, T. Chiu, "Electromagnetic scattering form slightly rough surfaces with inhomogeneous dielectric profiles", *IEEE Trans. on Antenna Propagat.*, vol. 45, no. 9, pp. 1419-1430, Sep. 1997.

[13] J. H. Richmond, "Scattering by thin dielectric strips", *IEEE Trans. on Antenna Propagat.*, vol. AP-33, no. 1, pp. 64-68, Jan. 1985.

[14] T. B. A. Senior, "Backscattering from resistive strips", *IEEE Trans. on Antenna Propagat.*, vol. AP-27, no. 6, pp. 808-813, Nov. 1979.

[15] R. Schiffer, K. O. Thielhein, "Light Scattering by dielectric needles and disks", *J. Appl. Physics*, vol. 50, no. 4, pp. 2476-2483, Apr. 1979.

고 일 석

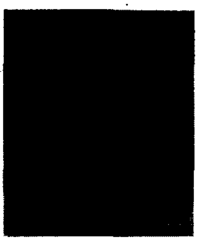

1992년 2월: 연세대학교 전자공학과 (공학사)
1994년 2월: 연세대학교 전자공학과 (공학석사)
1994년 1월~1996년 4월: LG 전자 연구원
2002년 8월: The University of Michigan at Ann Arbor 전기 및 전산과 (공학박사)
2004년 3월~현재: 인하대학교 정보통신대학원 교수
[주 관심분야] Theoretical Electromagnetic, Numerical Analysis, Channel Modeling